Mon. Not. R. Astron. Soc. **000**, 1–14 (2007) Printed 1 February 2008 (MN LaTeX style file v2.2)

arXiv:0707.4147v2 [astro-ph] 20 Sep 2007

The role of thermal evaporation in galaxy formation

Carlo Nipoti[1]⋆ and James Binney[2]
[1] *Dipartimento di Astronomia, Università di Bologna, via Ranzani 1, 40127 Bologna, Italy*
[2] *Rudolf Peierls Centre for Theoretical Physics, Keble Road, Oxford OX1 3NP, UK*

Accepted 2007 September 18. Received 2007 September 18; in original form 2007 July 27

ABSTRACT

In colour-magnitude diagrams most galaxies fall in either the “blue cloud” or the “red sequence”, with the red sequence extending to significantly brighter magnitudes than the blue cloud. The bright-end of the red sequence comprises elliptical galaxies with boxy isophotes and luminosity profiles with shallow central cores, while fainter elliptical galaxies have disky isophotes and power-law inner surface-brightness profiles. An analysis of published data reveals that the centres of galaxies with power-law central surface-brightness profiles have younger stellar populations than the centres of cored galaxies.

We argue that thermal evaporation of cold gas by virial-temperature gas plays an important role in determining these phenomena. In less massive galaxies, thermal evaporation is not very efficient, so significant amounts of cold gas can reach the galaxy centre and fill a central core with newly formed stars, consistent with the young stellar ages of the cusps of ellipticals with power-law surface-brightness profiles. In more massive galaxies, cold gas is evaporated within a dynamical time, so during an accretion event star formation is inhibited, and a core in the stellar density profile produced by dissipationless dynamics cannot be refilled. In this picture, the different observed properties of active galactic nuclei in higher-mass and lower-mass ellipticals are also explained because in the former the central supermassive black holes invariably accrete hot gas, while in the latter they typically accrete cold gas.

An important consequence of our results is that at the present time there cannot be blue, star-forming galaxies in the most massive galactic halos, consistent with the observed truncation of the blue cloud at $\sim L_*$.

Key words: conduction – galaxies: active – galaxies: elliptical and lenticular, cD – galaxies: formation – galaxies: structure

1 INTRODUCTION

Stars form from cold gas. Disk galaxies like the Milky Way or the Magellanic clouds have significant quantities of cold gas in their disks, and this gas has sustained star formation through most or all of the galaxies’ lifetimes. Elliptical galaxies lack cold gas, and for at least several gigayears these systems have not formed significant numbers of stars. Photometry of galaxies observed in the Sloan Digital Sky Survey shows that in a colour-magnitude diagram galaxies predominantly lie in either a “blue cloud” or a “red sequence”, with a smaller number of galaxies in a “green valley” between these features (Blanton et al. 2003; Baldry et al. 2004; Driver et al. 2006). Blue-cloud galaxies are forming stars, while red-sequence galaxies are not. Both populations extend to faint magnitudes, but the red sequence extends to significantly brighter magnitudes than the blue cloud.

Within the luminous elliptical galaxies of the red sequence two sub-populations can be distinguished. At very bright magnitudes there are objects with slightly boxy isophotes and luminosity profiles that become shallow at small radii, while at fainter magnitudes the galaxies mostly have disky isophotes and power-law inner surface-brightness profiles (Lauer et al. 1995; Faber et al. 1997; Graham, Erwin & Asensio Ramos 2003; Trujillo et al. 2004; Lauer et al. 2005; Ferrarese et al. 2006).

In this paper we argue that all these phenomena are reflections of the way gas at a galaxy’s virial temperature interacts with the cold gas required for star formation.

During an episode of star formation, only a part of the gas reservoir that drives the episode is converted into

---

⋆ E-mail: carlo.nipoti@unibo.it

stars; some of the residual gas is heated by supernovae to a temperature $\sim 3 \times 10^6$ K (Larson 1974; Dekel & Silk 1986). Dark halos with masses $\lesssim M_{\rm crit} \simeq 10^{12} M_\odot$ have potential wells that are too shallow to contain supernova-heated gas, so it flows out into intergalactic space. More massive halos do confine the hot gas gravitationally, with the result that once the halo's mass exceeds $M_{\rm crit}$, the density of hot gas in a halo builds up. As the density rises, the central cooling time of the gas shortens, and the rate at which gas accretes onto the central black hole (BH) increases. Studies of cooling flows suggest that the temperature sensitivity of the accretion rate onto the BH leads to an unsteady equilibrium, in which jets powered by accretion onto the BH replenish energy radiated by the gas (Birzan et al. 2004; Binney 2005). Hence halos with $M > M_{\rm crit}$ are filled with gas at the virial temperature, and the density of this gas steadily increases.

We argue that such trapped hot gas eliminates cold gas by a combination thermal conduction and ablation. In the more massive galaxies of the red sequence, cold gas is eliminated within a dynamical time, with the result that when an object that contains cold gas falls into such a galaxy, the infalling gas has negligible chance of reaching the galaxy's core before being heated to near the virial temperature. Hence, once a core develops in the luminosity profile of a massive galaxy of the red sequence, it cannot be be filled in by a central burst of star formation. A corollary is that these systems do not contain embedded disks, so their isophotes are more likely to be boxy than disky.

In less luminous galaxies of the red sequence, the time required for cold gas to be heated is likely to be longer than a dynamical time, so when one of these galaxies encounters a gas-rich system, there is a central burst of star formation that fills in the core in the luminosity profile that is produced by dissipationless dynamics. Moreover such central starbursts naturally account for the fact that elliptical galaxies with power-law inner luminosity profiles have younger central stellar populations (see Section 5.1).

The galaxies of the blue cloud are expected to contain hot gas – in the case of the Milky Way, Spitzer (1956) already made this inference – but such gas is typically not detected in X-ray observations, suggesting that its density is lower than in red-sequence galaxies of similar mass. Thus, evaporation of cold gas is not a significant process in blue-cloud galaxies. However, in the last decade it has become clear that star-forming disk galaxies cycle their interstellar media through their halos several times over the Hubble time (e.g. Fraternali & Binney 2006). Consequently, once a potential well becomes so deep that it confines supernova-heated gas, and gas accumulates at the virial temperature, the cycling of the interstellar gas through the halo makes the interstellar gas vulnerable to evaporation. Star formation ceases and the galaxy quickly moves from the blue cloud to the red sequence.

The paper is organised as follows. Section 2 defines the relevant parameters and presents formulae from which they can be calculated. Numerical values for representative galaxy models are presented in Section 3. When considering accretion events one has to add the effects of encounters with systems that vary widely in mass; Section 4 provides a treatment of this problem. Sections 5 and 6 discuss the implications for elliptical galaxies and galaxies of the blue cloud, respectively. Our conclusions are in Section 7.

Table 1. List of symbols. The shape factor is $A(\epsilon) = 1 - \epsilon$ (oblate spheroidal clouds) and $A(\epsilon) = (1-\epsilon)^2$ (prolate spheroidal clouds).

$a_{\rm sat}(r)$	Conduction saturated for cloud size $a < a_{\rm sat}$
$a_{\rm rad}(r)$	Cloud evaporates for cloud size $a < a_{\rm rad}$
$t_{\rm ev}(r)$	Evaporation time for cloud size $a < a_{\rm rad}$
$t_{\rm dyn}(r)$	Time to fall to the centre from r
$a_{\rm sf}(r)$	Minimum size of cloud that can reach centre from r
$M_{\rm rad}(r)$	Cloud mass for semi-major axis $a_{\rm rad}$: $\frac{4}{3}\pi A(\epsilon)\rho_{\rm c} a^3_{\rm rad}$
$M_{\rm sat}(r)$	Cloud mass for semi-major axis $a_{\rm sat}$: $\frac{4}{3}\pi A(\epsilon)\rho_{\rm c} a^3_{\rm sat}$
$M_{\rm sf}(r)$	Cloud mass for semi-major axis $a_{\rm sf}$: $\frac{4}{3}\pi A(\epsilon)\rho_{\rm c} a^3_{\rm sf}$
$M_{\rm min}$	$\max_{r>0} M_{\rm sf}(r)$

2 TIMESCALES FOR EVAPORATION

We want to determine the fate of a cloud of cool ($T_{\rm c} \ll 10^6$ K) gas that falls through gas at the virial temperature $T_{\rm ism} \sim 10^6 - 10^7$ K. In particular, we ask whether a spheroidal cloud with semi-major axis length a that is on a sufficiently low angular-momentum orbit can reach the galaxy centre and form stars there.

The motion of a cold cloud through a hot plasma is a complex dynamical process, involving heat conduction, radiative cooling, ram-pressure drag and ablation through the Kelvin-Helmholtz instability. We crudely simplify the treatment of this process by assuming that the cloud experiences only two opposed physical mechanisms: evaporation by thermal conduction from the hot interstellar medium (ISM) and condensation by radiative cooling.

The rate at which hot gas will ablate a cold cloud must depend on the speed of the cloud's motion through the ambient gas, and will be slowest for a stationary cloud; in this case a sheath of warm gas builds up around the cloud, partially insulating it from the hot ambient medium. In this paper we evaluate this minimum rate of ablation. We neglect the cloud's self-gravity, thus limiting ourselves to the case of clouds much smaller than the host galaxy.

Depending on the physical properties of the ISM and on the size (and geometry) of the cloud, the heat flux from the ISM to the cloud is either classical (Spitzer 1962) or saturated (Cowie & McKee 1977). For given temperature and density of the ISM, we define the 'saturation size' $a_{\rm sat}$ such that the heat flux saturates for $a \lesssim a_{\rm sat}$, and a 'critical size' $a_{\rm rad}$ at which radiative cooling balances heat conduction: clouds bigger than $a_{\rm rad}$ condense the ambient medium, while smaller clouds evaporate (McKee & Cowie 1977; Nipoti & Binney 2004, and references therein). For clouds of size $a \lesssim a_{\rm rad}$ we have to compare the evaporation time $t_{\rm ev}$ with the dynamical time $t_{\rm dyn}$. Only clouds for which $t_{\rm ev} > t_{\rm dyn}$ will survive long enough to form stars.

Let us consider, for simplicity, a spherical galaxy for which we know as functions of r, the electron temperature $T_{\rm ism}(r)$ and density $n_{\rm e,ism}(r)$ in the hot atmosphere. At each radius we can compute the critical size $a_{\rm rad}(r)$, and the evaporation time $t_{\rm ev}(a, r)$ of a cloud of size $a < a_{\rm rad}(r)$. At a given radius, the minimum size of a cloud for it to survive evaporation and end up forming stars is the "star-formation size" $a_{\rm sf}(r)$ such that $t_{\rm ev}(a_{\rm sf}, r) = t_{\rm dyn}(r)$. Clouds bigger than $a_{\rm sf}$ can reach the centre and there contribute to star formation. As the characteristic sizes are strongly dependent on the cloud geometry, it is more convenient to speak in terms of characteristic masses. Thus, for given cloud shape and average mass density, we define the masses $M_{\rm rad}$, $M_{\rm sat}$, $M_{\rm sf}$ of spheroidal clouds with semi-major axes $a_{\rm rad}$, $a_{\rm sat}$, $a_{\rm sf}$, respectively. To form stars in the central regions, an infalling cloud must survive evaporation at all radii, so only clouds more massive than $M_{\rm min} = \max_{r>0} M_{\rm sf}(r)$ can contribute to central star formation. We will refer to $M_{\rm min}$ as the "minimum cloud mass", because in a given galaxy all clouds less massive than $M_{\rm min}$ will be evaporated and absorbed by the ISM within a dynamical time. Table 1 lists these definitions.

2.1 Calculation of evaporation times

Following Cowie & Songaila (1977), we consider gas clouds modelled as prolate and oblate spheroids, which can represent a wide range of geometries, from filaments to disks, through spherical clouds. We consider oblate and prolate spheroidal coordinates (u, v) related to the cylindrical coordinates (R, z) by $R = \Delta \cosh u \sin v$, $z = \Delta \sinh u \cos v$ (oblate), and $R = \Delta \sinh u \sin v$, $z = \Delta \cosh u \cos v$ (prolate), where Δ is a length scale. The cloud is a prolate or oblate spheroid with surface $u = u_0$. The semi-major and semi-minor axes of the cloud surface are[1] $a = \Delta \cosh u_0$ and $b = \Delta \sinh u_0$, and the cloud ellipticity is $\epsilon \equiv 1 - b/a = 1 - \tanh u_0$. We assume that in the interface the electron temperature and density are stratified with u. At the cloud surface ($u = u_0$), the electron temperature is $T_{\rm c} \ll T_{\rm ism}$, while $T \to T_{\rm ism}$ for $u \to \infty$.

In the regime of unsaturated heat conduction ($a > a_{\rm sat}$), the heat flux is given by the classical Spitzer formula

$$\mathbf{q}_{\rm cl} = -\kappa(T)\nabla T, \tag{1}$$

where the thermal conductivity is

$$\kappa(T) = f\kappa_0 T^{5/2}, \tag{2}$$

where $\kappa_0 \simeq 1.84 \times 10^{-5} (\ln\Lambda)^{-1}\,{\rm erg\,s^{-1}\,cm^{-1}\,K^{-7/2}}$ (Spitzer 1962), $f \leq 1$ is the factor by which magnetic fields suppress thermal conduction (e.g. Binney & Cowie 1981; Böhringer & Fabian 1989; Tribble 1989), and $\ln\Lambda$ is the Coulomb logarithm, which is only weakly dependent on $n_{\rm e}$ and T (in the following we assume $\ln\Lambda = 30$). In the regime of classical heat conduction and negligible radiative cooling ($a_{\rm sat} < a < a_{\rm rad}$), Cowie & Songaila (1977) computed analytically the evaporation rate of prolate and oblate clouds of cold ($T_{\rm c} \sim 0$) gas immersed in a medium of temperature $T_{\rm ism}$: the evaporative mass loss rate is

$$\dot{M} = \frac{16\pi f \mu m_{\rm p} \kappa_0 T_{\rm ism}^{5/2} \Delta}{25 k_{\rm B} B(\epsilon)}, \tag{3}$$

where μ is the mean gas particle mass in units of the proton mass $m_{\rm p}$, $k_{\rm B}$ is the Boltzmann constant, $B(\epsilon) = \frac{\pi}{2} - 2\arctan[\tanh(u_0/2)]$ (oblate) and $B(\epsilon) = |\ln[\tanh(u_0/2)]|$ (prolate), with $u_0 = {\rm arctanh}(1-\epsilon)$. In the spherical limit $\epsilon \to 0$ ($u_0 \gg 1$), equation (3) yields the mass loss rate of a spherical cloud with radius a (Cowie & McKee 1977). Given the average mass density of clouds $\rho_{\rm c}$, the mass of a cloud of semi-major axis a is

$$M = \frac{4}{3}\pi A(\epsilon) a^3 \rho_{\rm c} \simeq \tag{4}$$

$$\simeq 1.3 \times 10^8 A(\epsilon) \left(\frac{a}{\rm kpc}\right)^3 \left(\frac{n_{\rm H,c}}{\rm cm^{-3}}\right) M_\odot,$$

where $A(\epsilon) = 1-\epsilon$ (oblate) or $A(\epsilon) = (1-\epsilon)^2$ (prolate), $n_{\rm H,c}$ is the cloud hydrogen density, and when deriving the numerical value we have used $\rho_{\rm c} \simeq 1.3 m_{\rm p} n_{\rm H,c}$ (appropriate for abundances $Y = 0.25$, $X = 0.75$). Combining equations (3) and (4), we get the evaporation time

$$t_{\rm ev}(a,r) \equiv \frac{M}{\dot{M}} = \frac{25 k_{\rm B} \rho_{\rm c} a^2 C(\epsilon)}{12 f \kappa_0 \mu m_{\rm p} T_{\rm ism}^{5/2}} \simeq \tag{5}$$

$$\simeq 9.9 \times 10^2 \frac{C(\epsilon)}{f} \left(\frac{n_{\rm H,c}}{\rm cm^{-3}}\right) \left(\frac{T_{\rm ism}}{10^7\,{\rm K}}\right)^{-5/2} \left(\frac{a}{\rm kpc}\right)^2 \;{\rm Myr},$$

where $C(\epsilon) \equiv A(\epsilon)B(\epsilon)\cosh[{\rm arctanh}(1-\epsilon)]$, and we have used $\mu = 0.59$. The time for a cloud to fall to the centre from r is the dynamical time[2]

$$t_{\rm dyn}(r) = \sqrt{\frac{3\pi}{16 G \bar{\rho}_{\rm dyn}}} \simeq \tag{6}$$

$$\simeq 7.44 \left(\frac{r}{\rm kpc}\right)^{3/2} \left[\frac{M_{\rm dyn}(r)}{10^{10} M_\odot}\right]^{-1/2} \;{\rm Myr},$$

where $\bar{\rho}_{\rm dyn}(r) = 3M_{\rm dyn}(r)/4\pi r^3$ is the average mass density within r (e.g. Binney & Tremaine 1987). From equation (5) and from the condition $t_{\rm ev}(a_{\rm sf}, r) = t_{\rm dyn}(r)$, we derive the star-formation size

$$a_{\rm sf} \simeq 0.32 \left(\frac{f}{C(\epsilon)} \frac{t_{\rm dyn}}{10^8\,{\rm yr}}\right)^{1/2} \left(\frac{n_{\rm H,c}}{\rm cm^{-3}}\right)^{-1/2} \left(\frac{T_{\rm ism}}{10^7\,{\rm K}}\right)^{5/4} {\rm kpc}. \tag{7}$$

As pointed out above, equation (7) holds only if $a_{\rm sat} < a_{\rm sf} < a_{\rm rad}$. Postponing to Appendix A a detailed treatment of the effects of saturation and radiation in the evaporation of spheroidal clouds, we report here the equations relating $a_{\rm sat}$ and $a_{\rm rad}$ to the physical properties of the ISM. The saturation size is (Cowie & McKee 1977; Cowie & Songaila 1977)

$$a_{\rm sat} = 5.0 \times 10^{-4} \frac{f^{1/2}\cosh u_0}{\tilde{\sigma}_{0,\rm sat}\phi_{\rm sat}} \left(\frac{T_{\rm ism}}{10^7\,{\rm K}}\right)^2 \left(\frac{n_{\rm e,ism}}{\rm cm^{-3}}\right)^{-1} {\rm kpc}, \tag{8}$$

where $\phi_{\rm sat} \sim 1$ and $\tilde{\sigma}_{0,\rm sat}(\epsilon)$ are dimensionless parameters ($0.05 \lesssim \tilde{\sigma}_{0,\rm sat} \lesssim 1$ for $0.99 \gtrsim \epsilon \gtrsim 0$, see Appendix A1). In the case of significant saturation ($a < a_{\rm sat}$), we should solve the equations for saturated heat conduction. As pointed out by Cowie & Songaila (1977), the only analytic solution is for spherical symmetry (see equation A6), while in prolate or oblate geometry a two-dimensional partial differential equation must be solved numerically. However, when $a < a_{\rm sat}$ the evaporation time-scale computed for unsaturated thermal conduction provides a lower limit (and the corresponding star-formation size $a_{\rm sf}$ an upper limit), and we shall see that these limits together with the analytic solution for the spherical case provide sufficient constraints for our purposes.

In spherical symmetry, the critical size at which the cloud is radiatively stabilised is (McKee & Cowie 1977)

$$a_{\rm rad} = 1.9 \times 10^{-2} \frac{f^{1/2}}{\phi_{\rm sat}} \left(\frac{T_{\rm ism}}{10^7\,{\rm K}}\right)^2 \left(\frac{n_{\rm e,ism}}{\rm cm^{-3}}\right)^{-1} {\rm kpc}. \tag{9}$$

---

[1] Note the different notation: here a is the semi-major axis, while in Cowie & Songaila (1977) a is the scale-length (our Δ).

[2] The actual time will be somewhat longer because of the drag force (See Appendix B for a discussion).

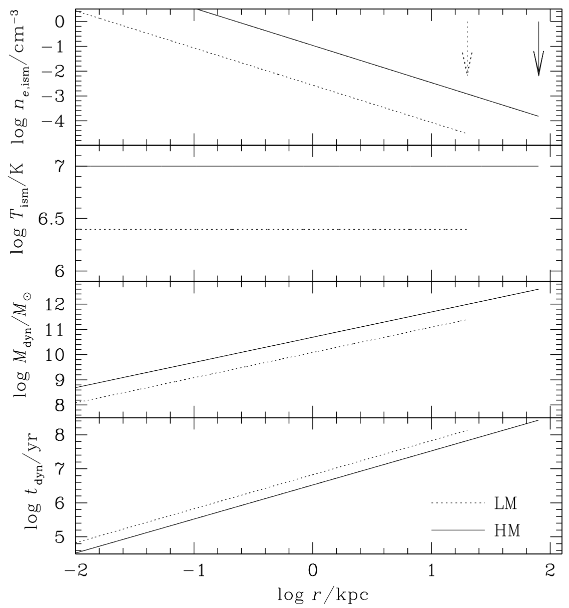

Figure 1. From top to bottom: electron density and temperature of the ISM, dynamical mass and dynamical time as functions of radius for the galaxy models LM (dotted lines) and HM (solid lines). The arrows indicate the bounding radii $r_{\rm max}$ of the two models.

Out of spherical symmetry the critical size cannot be computed analytically. However, we assume $a_{\rm rad}$ as derived above to be approximately correct also for oblate and prolate spheroids (see Appendix A2 for a discussion).

Summarising, at each radius in a galaxy we have three characteristic cloud masses: the star-formation mass $M_{\rm sf}$, the saturation mass $M_{\rm sat}$, and the mass of radiatively stabilised clouds $M_{\rm rad}$. For given ϵ and $n_{\rm H,c}$ these masses are computed from equation (4), using the values of $a_{\rm sf}$, $a_{\rm sat}$ and $a_{\rm rad}$ from equations (7), (8) and (9). Provided that $M_{\rm sat} < M_{\rm sf} < M_{\rm rad}$, the maximum of $M_{\rm sf}$ over all radii represents the minimum mass $M_{\rm min}$ of a cool cloud that will survive evaporation long enough to contribute to a central starburst. If at any radius $M_{\rm sf} > M_{\rm rad}$, our neglect of cooling is invalid; then we must assume $M_{\rm sf} = M_{\rm rad}$, because clouds more massive than $M_{\rm rad}$ condense the ambient medium. On the other hand, if $M_{\rm sf} < M_{\rm sat}$, $M_{\rm sf}$ is just an upper limit to the actual value of the star-formation mass. At a given radius r, the characteristic masses $M_{\rm sf}$, $M_{\rm sat}$ and $M_{\rm rad}$ scale with the suppression factor as $f^{3/2}$, and depend on ϵ and $n_{\rm H,c}$. The value of $n_{\rm H,c}$ can be constrained because we expect that the cloud is either in pressure equilibrium with the ambient medium or overpressured (either by gravity or supernova-driven expansion). In particular, we consider here clouds at $T_{\rm c} \sim 10^4\,{\rm K}$ with hydrogen density $n_{\rm H,c} = \max[0.86 n_{\rm e,ism}(T_{\rm ism}/10^4\,{\rm K}), 1\,{\rm cm}^{-3}]$.

3 CLOUD MASSES IN ELLIPTICALS

Many elliptical galaxies have diffuse soft X-ray emission from a hot atmosphere. In this section we investigate how such an atmosphere affects the fate of any cold gas that might fall into the galaxy, for example during a merger.

Table 2. Parameters of the model galaxies LM (low mass) and HM (high mass). $M_{\rm gal}$: baryonic mass. $M_{\rm dyn,tot}$: total dynamical mass. T_0: electron temperature of the ISM. $n_{\rm e,0}$: electron number density of the ISM at $r = 1\,{\rm kpc}$. $r_{\rm max}$: bounding radius.

Model	$M_{\rm gal}$ $M_{\odot}$	$M_{\rm dyn,tot}$ $M_{\odot}$	T_0 K	$n_{\rm e,0}$ cm^{-3}	$r_{\rm max}$ kpc
LM	3.0×10^{10}	2.5×10^{11}	2.5×10^6	2.7×10^{-3}	20
HM	3.0×10^{11}	3.9×10^{12}	1.0×10^7	1.1×10^{-1}	80

Detailed radial temperature and density profiles are available for only a few, mostly exceptionally luminous galaxies (Irwin & Sarazin 1996; Mathews & Brighenti 2003; Humphrey et al. 2006; Fukazawa et al. 2006; David et al. 2006; Randall, Sarazin & Irwin 2006; O'Sullivan, Sanderson & Ponman 2007). While it is straightforward to evaluate the parameters of Table 1 for specific galaxies that have observationally estimated profiles, it is more instructive to use the data to build representative model galaxies and evaluate the quantities of Table 1 for these models.

Our models are spherical and within some bounding radius $r_{\rm max}$ have perfectly flat circular-speed curves, so the total dynamical mass interior to r is $M_{\rm dyn}(r)/M_{\rm dyn,tot} = r/r_{\rm max}$, where $M_{\rm dyn,tot} \equiv M_{\rm dyn}(r_{\rm max})$. We take the ISM to be in hydrostatic equilibrium at a constant temperature $T_{\rm ism}(r) = T_0$. From these assumptions it follows that the density profile of the gas is a power law in r with a slope that depends on T_0; we adopted

$$n_{\rm e,ism}(r) = \begin{cases} n_{\rm e,0}(r/\,{\rm kpc})^{-3/2} & r < r_{\rm max} \\ 0 & \text{otherwise.} \end{cases}$$

We consider two models, the parameters of which are reported in Table 2: model LM represents a relatively low-mass, gas-poor elliptical galaxy such as NGC 3377 or NGC 3245, while model HM represents a high-mass, gas-rich elliptical galaxy such as NGC 4472 or NGC 4649. $M_{\rm dyn}(r)$, $n_{\rm e,ism}(r)$, $t_{\rm dyn}(r)$, and $T_{\rm ism}(r)$ are plotted in Fig. 1 for models LM (dotted lines) and HM (solid lines).

For models LM and HM we computed the characteristic masses $M_{\rm rad}(r)$, $M_{\rm sf}(r)$, $M_{\rm sat}(r)$ and $M_{\rm min}$ for oblate and prolate cloud models with ellipticity in the range $0 < \epsilon < 0.99$. In all cases (even for thermal conduction suppression factor $f \sim 1$) we find $a_{\rm sf}(r) \ll r$, where $a_{\rm sf}(r)$ is the size of a cloud of mass $M_{\rm sf}(r)$, consistent with our assumption of small clouds. Figure 2 shows the characteristic masses (in units of $f^{3/2} M_{\odot}$) as functions of radius for models HM (top panels) and LM (bottom panels) for three representative cloud shapes: gas filaments (prolate cloud with $\epsilon = 0.98$; left), spherical gas clouds (centre), and gas disks (oblate cloud with $\epsilon = 0.98$; right). Figure 3 plots $M_{\rm min}$ as a function of ϵ for prolate and oblate clouds, for model HM (region shaded with red vertical lines) and LM (region shaded with blue diagonal lines). We checked these results by evaluating the parameters of the gas rich galaxies NGC 4472 and NGC 4649 (Irwin & Sarazin 1996; Humphrey et al. 2006; Randall, Sarazin & Irwin 2006), and the gas-poor galaxies NGC 3377 and NGC 3245 (David et al. 2006), finding results similar to those of the models LM and HM, respectively. Figs. 2 and 3 yield the following conclusions:

- The star-formation mass $M_{\rm sf}$ is an increasing function

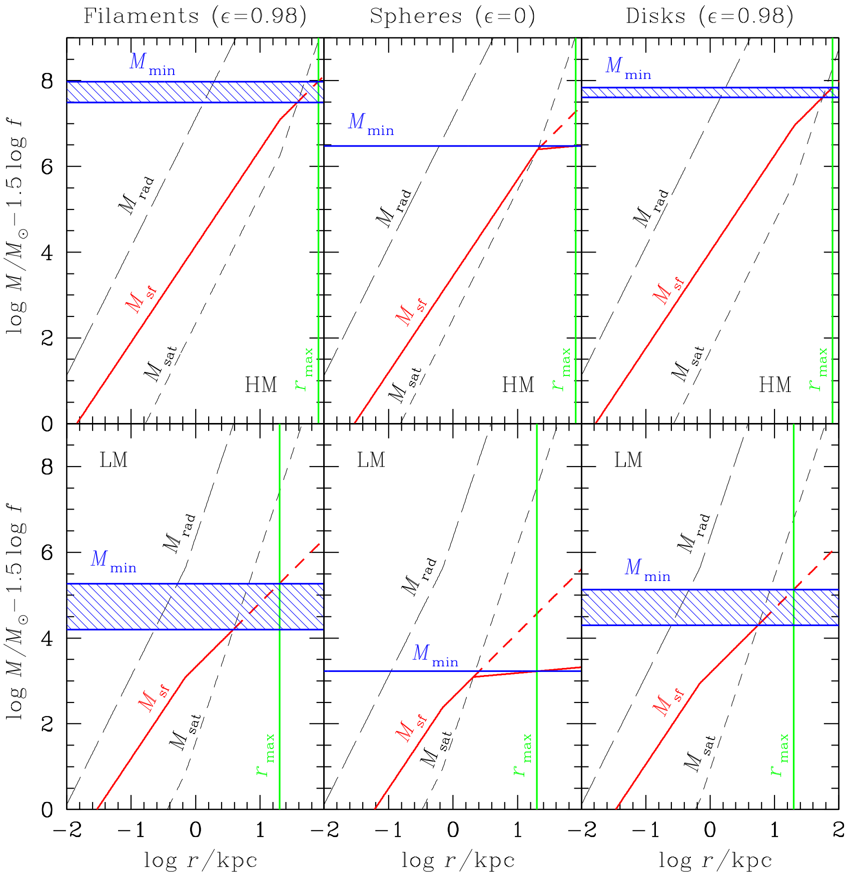

Figure 2. Characteristic cloud masses for models HM (top) and LM (bottom), for gas filaments (left), spherical clouds (centre), and gas disks (right). In each panel, the minimum mass $M_{\rm min}$ (blue) is the maximum of $M_{\rm sf}$ (red) over all radii smaller than $r_{\rm max}$ (green); the dashed red line represents an upper limit of $M_{\rm sf}$; the blue shaded region represents values of M between the lower and upper limit of $M_{\rm min}$; the black curves correspond to $M = M_{\rm rad}$ (long dashed), and $M = M_{\rm sat}$ (short dashed). Masses are in units of $f^{3/2} M_\odot$, where f is the factor by which thermal conduction is reduced below the Spitzer value.

of radius, partly because the dynamical time is and partly because of its dependence on $n_{\rm H,c}$. This indicates that cool clouds are more vulnerable in the outer regions of the galaxy. We note that in Fig. 2 the change of slope of the curves representing $M_{\rm rad}(r)$, $M_{\rm sat}(r)$ and $M_{\rm sf}(r)$ reflects the transition between overpressured clouds ($n_{\rm H,c} = 1\,{\rm cm}^{-3}$; outer regions) and clouds in pressure equilibrium ($n_{\rm H,c} > 1\,{\rm cm}^{-3}$; inner regions; see Section 2.1).

- In all cases $M_{\rm rad}$ is significantly higher than $M_{\rm sf}$, so neglecting radiative cooling in the computation of $a_{\rm sf}$ is justified.

- Saturation becomes important at large radii, where the density of the ISM becomes low. So $M_{\rm sf}$ at large radii is just an upper limit (dashed red lines in Fig. 2) and, as a consequence, only upper and lower limits on $M_{\rm min}$ can be derived (shaded blue areas in Fig. 2). An exception is the spherical case, for which we computed $M_{\rm sf}$ also in the saturated regime, by using as evaporation time $M/\dot{M}_{\rm sat}$, with $\dot{M}_{\rm sat}$ given in equation (A6). From Fig. 2 (central column of panels) it is apparent that $M_{\rm sf}(r)$ for spherical clouds is almost constant in the saturated regime. As a consequence, $M_{\rm min}$ (solid symbols in Fig. 3) lies close to the lower limit one would derive from the classical evaporation rate. This suggests that also in the case of prolate and oblate clouds the actual value of $M_{\rm min}$ should be closer to the lower than to the upper limit. So, we expect the actual value of $M_{\rm min}$ to be basically independent of $r_{\rm max}$.

- For given model galaxy, $M_{\rm min}$ depends on the geometry of the cloud, with higher values obtained for very non-spherical systems (especially filaments) and the lowest values obtained in the case of spherical clouds (see Fig. 3). Thus for fixed mass, more non-spherical systems are more vulnerable to evaporation.

- For fixed cloud geometry, $M_{\rm min}$ is (in physical units) typically about three orders of magnitude higher in model HM than in model LM (Fig. 3). More significantly, $M_{\rm min}$ normalised to the baryonic mass of the galaxy $M_{\rm gal}$ is a factor of ~ 100 higher in model HM than in model LM. Thus, proportionally bigger clouds are eliminated by evaporation in model HM than in model LM.

- The actual value of $M_{\rm min}$ in physical units is largely uncertain because of the dependence on $f^{3/2}$. In the (unlikely) case of Spitzer conductivity ($f \sim 1$) we get $M_{\rm min} \sim 10^7 - 10^8 M_\odot$ in model HM and $M_{\rm min} \sim 10^4 - 10^5 M_\odot$ in

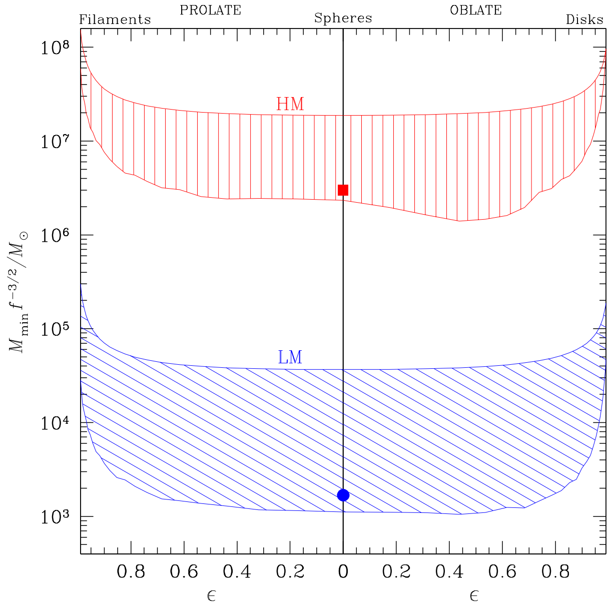

Figure 3. Minimum mass as a function of ϵ for prolate (left) and oblate (right) clouds in units of $f^{3/2}M_\odot$. The minimum mass lies in the region shaded with red vertical lines for model HM and in the region shaded with blue diagonal lines for model LM. The solid red square and blue circle indicate the values of $M_{\rm min}$ obtained for spherical clouds for model HM and LM, respectively.

model LM, but for a more plausible value of the suppression factor, $f \sim 0.01$ (Nipoti & Binney 2004, and references therein), $M_{\rm min}$ is as low as $M_{\rm min} \sim 10^4 - 10^5 M_\odot$ in model HM and $M_{\rm min} \sim 10 - 100 M_\odot$ in model LM.

4 AGGREGATE GAS INFALL

The quantity $M_{\rm min}$ is the minimum mass an individual cloud must have to survive infall to the centre. To estimate the mass of cold gas that becomes available for central star formation, we need to integrate over the spectrum of cloud masses from this minimum mass to infinity. We can only guess at the form of the spectrum. Clearly it reflects the baryonic-mass spectrum of galaxies that are available to be captured by the galaxy under study, which might be approximated by the baryonic-mass function of all galaxies truncated at the baryonic mass of the given galaxy to take account of the fact that an encounter with a more massive galaxy leads to destruction rather than growth. In reality this spectrum will overemphasise big clouds, both because no galaxy has more than a small fraction of its mass in cold gas, and because tidal shredding will split a galaxy into many clouds during a merger. Therefore a reasonable hypothesis for the cloud spectrum is the baryonic mass spectrum of galaxies first truncated at the mass of the given galaxy and then scaled to smaller masses by a factor β in the range $(0.01, 0.1)$.

If we identify the baryonic-mass function with the luminosity function, and approximate the latter with the Schechter (1976) form, the mass of cold gas that can reach the centre of a galaxy of baryonic mass $M_{\rm gal}$ is

$$M_{\rm acc} \propto M_* \int_{M_{\rm min}/\beta M_*}^{M_{\rm gal}/M_*} {\rm d}x\, x^{1-\alpha} {\rm e}^{-x}, \qquad (10)$$

where $\alpha \simeq 1.25$ is the faint-end slope of the Schechter function, and $M_* \simeq 10^{11} M_\odot$ is the baryonic mass of an L_* galaxy. The integrand above varies slowly below the exponential cutoff, so we can approximate the integral by the between its lower limit and the smaller of the upper limit and unity. Then the dimensionless measure of the importance of cold accretion is

$$\frac{M_{\rm acc}}{M_{\rm gal}} \propto \begin{cases} \min\left(1, \frac{M_*}{M_{\rm gal}}\right) - \frac{M_{\rm min}}{\beta M_{\rm gal}} & \frac{M_{\rm min}}{\beta M_{\rm gal}} < \min\left(1, \frac{M_*}{M_{\rm gal}}\right) \\ 0 & \text{otherwise.} \end{cases} \qquad (11)$$

Thus accretion shuts off completely for $M_{\rm min} > \beta \min(M_{\rm gal}, M_*)$, and for $M_{\rm gal} > M_*$ its importance declines faster than $M_{\rm gal}^{-1}$.

Since we require the mass function of gas-rich objects rather than the luminosity function of galaxies, it is not clear that it is appropriate to obtain α from the galaxy luminosity function: at early times the spectrum of cloud masses should be the same as the spectrum of dark-matter halos, which has a steeper slope $\alpha \simeq 2$. The flatter spectrum of the galaxy luminosity function is thought to arise from the difficulty of forming stars in low-mass halos, not from an absence of low-mass gas clouds. If we take $\alpha = 2$, the integral above should be approximated by

$$\int_{x_0}^{x_1} {\rm d}x\, x^{-1} {\rm e}^{-x} \simeq \begin{cases} \ln[\min(1, x_1)/x_0] & x_0 < \min(1, x_1) \\ 0 & \text{otherwise} \end{cases} \qquad (12)$$

so

$$\frac{M_{\rm acc}}{M_{\rm gal}} \propto \begin{cases} \frac{M_*}{M_{\rm gal}} \ln\left[\frac{\beta M_{\rm gal}}{M_{\rm min}} \min\left(1, \frac{M_*}{M_{\rm gal}}\right)\right] & \frac{M_{\rm min}}{\beta M_{\rm gal}} < \min\left(1, \frac{M_*}{M_{\rm gal}}\right) \\ 0 & \text{otherwise.} \end{cases} \qquad (13)$$

Again cold accretion declines in importance faster than $M_{\rm gal}^{-1}$ and cuts off for $M_{\rm min} > \beta \min(M_{\rm gal}, M_*)$.

Figure 4 shows the relative importance for the LM and HM models of cold accretion from a spectrum of cloud masses. The full curves apply if the latter has the same low-end slope as the mass spectrum of cold dark matter (CDM) halos, while the dashed curves apply if the low-end slope of the cloud spectrum is the same as that of the galaxy luminosity function. In each case, two curves are plotted, showing the extreme cases of only spherical clouds (thick lines) and only filaments[3] (thin lines). When $1.5 \log f - \log \beta < 2$, the relative importance of accretion in the LM and HM models is nearly independent of f, β and geometry but increases with α. Thus accretion will have the biggest differential impact on LM and HM systems when the low-end slope of the mass spectrum of clouds is steep. If $1.5 \log f - \log \beta > 2$, either because conductivity is efficient or clouds fragment strongly during mergers, accretion cuts off in HM systems and the ratio plotted in Fig. 4 shoots upwards. Accretion cuts off for smaller values of f is clouds are filamentary.

In summary, the importance of cold accretion, measured by $M_{\rm acc}/M_{\rm gal}$, depends on the assumptions on the cloud mass spectrum and on the highly uncertain parameters f and β. If $1.5 \log f - \log \beta \lesssim 2$, $(M_{\rm acc}/M_{\rm gal})_{\rm LM}/(M_{\rm acc}/M_{\rm gal})_{\rm HM}$ will lie the range $3 - 30$. If

---

[3] In this case we used as $M_{\rm min}$ the lower limit found for $\epsilon = 0.98$ prolate clouds.

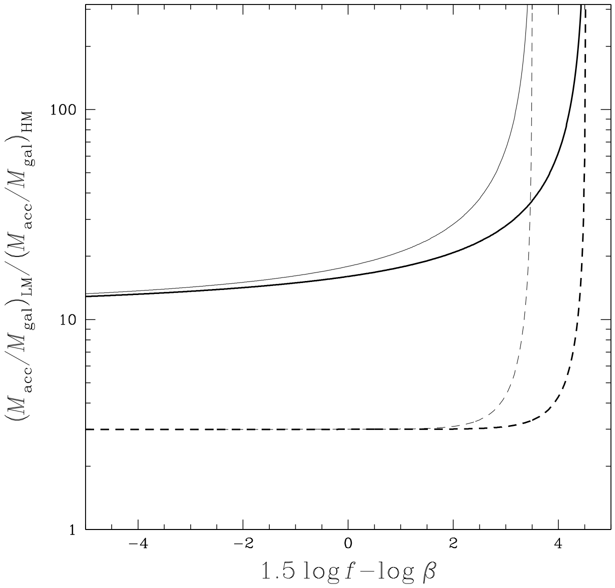

Figure 4. The ratio between the quantity $M_{\rm acc}/M_{\rm gal}$ in the LM model galaxy and the same quantity in the HM model galaxy as a function of the efficiency of thermal conduction f and of the parameter β defined in Section 4 ($M_{\rm acc}$ is the mass of accreted cold gas that can reach the galaxy centre and $M_{\rm gal}$ is the baryonic mass of the galaxy). The full curves apply if the cloud mass spectrum has the same low-end slope as the mass spectrum of CDM halos, while the dashed curves apply if the slope is that of the galaxy luminosity function. Thick and thin curves refer to spherical clouds and filaments, respectively.

processes such as the Kelvin-Helmholtz instability are effective in breaking clouds into small fragments, $1.5\log f - \log\beta$ could take on larger values and accretion would be suppressed in HM systems.

5 IMPLICATIONS FOR ELLIPTICALS

Figures 3 and 4 show that in an X-ray luminous galaxy a cold cloud has to be $\sim 10^3$ times more massive to reach the centre than in an elliptical with weak X-ray emission, and aggregate gas in infall available for central star formation is more important in the latter than in the former. Thus we expect cold gas and its associated star formation to have a much bigger impact on the centres of X-ray weak ellipticals than on the centres of their X-ray luminous brethren. In this section we discuss the nature of this impact and relate it to a dichotomy in the observed properties of elliptical galaxies.

5.1 Observed properties of power-law and core galaxies

On the basis of their central surface brightness (SB) profiles, luminous elliptical galaxies fall into two distinct classes: power-law (or Sersic) galaxies (PLGs), with SB profiles well represented by the Sersic (1968) law down to the centre, and core (or core-Sersic) galaxies (CGs), with SB profiles deviating from the Sersic law in the central regions because of the presence of a flat core (Lauer et al. 1995; Faber et al. 1997; Graham, Erwin & Asensio Ramos 2003; Trujillo et al. 2004; Lauer et al. 2005; Ferrarese et al. 2006). Quantitatively, the corresponding intrinsic stellar density profiles have inner logarithmic slope $\gamma > 0.5$ in PLGs, and $\gamma < 0.3$ in CGs, with few "intermediate" galaxies, having $0.3 < \gamma < 0.5$ (Ravindranath et al. 2001; Rest et al. 2001; Lauer et al. 2007). It is useful to summarise the main observed properties of PLGs and CGs.

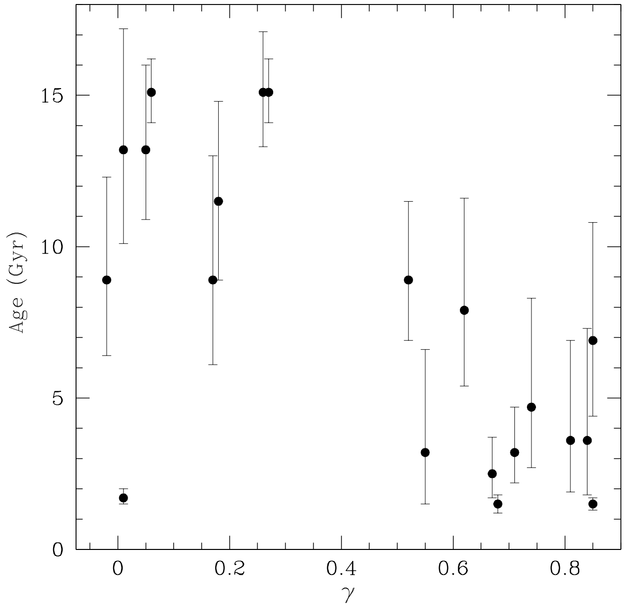

Figure 5. The age of the central stellar population versus the central slope of the SB profile γ for a subsample of the elliptical and lenticular galaxies studied by McDermid et al. (2006). Central ages (with error bars) are from McDermid et al. (2006), while the values of γ are from Lauer et al. (2007).

(i) *Global galaxy properties:*

(a) CGs are typically more luminous than PLGs, with a dividing luminosity $L_{\rm V} \sim 3\times10^{10}L_{{\rm V}\odot}$. In particular, all galaxies brighter than $L_{\rm V} \sim 5\times10^{10}L_{{\rm V}\odot}$ are CGs, while all galaxies fainter than $L_{\rm V} \sim 2\times10^{10}L_{{\rm V}\odot}$ are PLGs. At intermediate luminosities both types coexist (Faber et al. 1997; Lauer et al. 2007).

(b) CGs have boxy isophotes and rotate slowly, PLGs have disky isophotes and rotate rapidly (Kormendy & Bender 1996; Faber et al. 1997).

(c) Almost all the brightest cluster galaxies are CGs (Laine et al. 2003).

(d) All galaxies with high X-ray emission from hot gas (high $L_{\rm X}/L_{\rm B}$) are CGs, while ellipticals with lower $L_{\rm X}/L_{\rm B}$ include both CGs and PLGs (Pellegrini 1999, 2005; Ellis & O'Sullivan 2006).

(ii) *Properties of the central regions:*

(a) All ellipticals have central colour gradients, becoming redder towards the centre. CGs have weaker central colour gradients than do PLGs, though the difference is small and there is large scatter (Lauer et al. 2005).

(b) CGs are rounder than PLGs at small radii. PLGs typically have central stellar disks, while CGs do not (Lauer et al. 2005).

(c) Nuclei (typically bluer than the surrounding galaxy) are more frequent in PLGs than in CGs (Lauer et al. 2005). In the Virgo cluster no galaxies brighter than $L_{\rm B} \sim 2.5 \times 10^{10} L_{\rm B\odot}$ have nuclei (Côté et al. 2006; Ferrarese et al. 2006).

(d) Lower-velocity dispersion ellipticals have significantly younger central stellar populations than higher-velocity dispersion ellipticals (McDermid et al. 2006, and references therein). This should imply a correlation between the stellar age of the inner regions of ellipticals and the central slope γ of the SB profile. Combining information on the central age from McDermid et al. (2006) and on γ from Lauer et al. (2007), we considered a sample of 20 elliptical and lenticular galaxies, which turn out to be nicely segregated in a diagram plotting central age versus γ (Fig. 5), with CGs and PLGs having median central ages 13.2 Gyr and 3.6 Gyr, respectively[4].

(iii) *Activity of the central black hole:*

(a) The mean ratio $L_{\rm opt,nuc}/L_{\rm Edd}$ of the optical nuclear emission and the Eddington luminosity of the central BH is higher by two orders of magnitude in PLGs than in CGs (Capetti & Balmaverde 2006).

(b) If $P_{1.4}$ is the global power of both core and extended emission at 1.4 GHz CGs cover the full range ($18 \lesssim \log P_{1.4}/W{\rm Hz}^{-1} \lesssim 26$), while PLGs show no significant radio activity (de Ruiter et al. 2005).

(c) With $R = L_{\rm 5GHz,nuc}/L_{\rm B,nuc}$ the ratio of the radio to B-band luminosities of the nucleus and $R_X = L_{\rm 5GHz,nuc}/L_{\rm HX,nuc}$ the ratio of radio and $2-10$ keV X-ray luminosities, CGs are radio-loud ($\log R \sim 3.6$; $\log R_X \sim -1.3$), while PLGs are radio-quiet ($\log R \sim 1.6$; $\log R_X \sim -3.3$) (Capetti & Balmaverde 2006; Balmaverde & Capetti 2006).

5.2 Formation mechanisms of the central stellar profiles

During hierarchical galaxy formation luminous galaxies arise from mergers of lower-luminosity systems. Lower-luminosity galaxies tend to be PLGs, so the natural starting point for discussing the origin of the CG/PLG dichotomy is the morphology of PLGs. That is, we assume that at early enough times any elliptical galaxy is a PLG, and our task is to explain why some systems became CGs. In this spirit one associates with each CG a mass deficit $M_{\rm def}$ equal to the mass that would have to be added to the core to make the SB profile that of a PLG: typically $M_{\rm def} \sim M_{\rm bh}$, where $M_{\rm bh}$ is the central BH mass (Milosavljevic et al. 2002; Graham 2004; Merritt 2006). This observation suggests the following popular "core-scouring" scenario, which has been validated by N-body simulations (Milosavljevic & Merritt 2001)[5]: during dissipationless merging, the orbiting BHs reduce the central star density by scattering stars out of the most tightly bound orbits (Begelman, Blandford & Rees 1980; Ebisuzaki, Makino & Okumara 1991; Makino & Ebisuzaki 1996; Faber et al. 1997; Quinlan & Hernquist 1997; Volonteri, Madau & Haardt 2003). Thus in the core-scouring scenario the central slope γ is determined by the merging history of the galaxy, and the mass deficit $M_{\rm def}$ is naturally of the order of the masses of the participating BHs. The core-scouring scenario is successful in reproducing some of the observations, but it cannot be a complete explanation[6] because no purely stellar-dynamical mechanism can introduce a characteristic mass scale and thus explain why PLGs are never luminous, while CGs often are. Moreover, core scouring alone does not explain the origin of the correlation between the presence of cores and strong diffuse X-ray emission (Pellegrini 2005; Ellis & O'Sullivan 2006), nor does it explain why flat cores have not formed in PLGs, given that low-luminosity ellipticals such as M32 also harbour BHs (Faber et al. 1997).

5.3 The role of thermal evaporation in determining the power-law/core dichotomy

The discussion above suggests that a plausible working hypothesis is that all ellipticals at some stage in their evolution have central cores. The results of Sections 3 and 4 and the relative youth of the central regions of PLGs (Fig. 5) suggest that in PLGs the core created by dissipationless dynamics has been filled in by star formation from cold gas that fell in during or after a merger. The aggregate mass of new stars formed will be proportional to the quantity $M_{\rm acc}$ introduced in Section 4. The proposal requires that $M_{\rm acc} \gtrsim M_{\rm def}$ in PLGs and $M_{\rm acc} < M_{\rm def}$ in CGs. We know that $M_{\rm def} \sim M_{\rm bh}$, and $M_{\rm bh}$ is proportional to the total stellar mass of the galaxy (Magorrian et al. 1998; Marconi & Hunt 2003), so it is reasonable to assume $M_{\rm def} \propto M_{\rm gal}$. So $M_{\rm acc}/M_{\rm def} \propto M_{\rm acc}/M_{\rm gal}$, and our finding that $M_{\rm acc}/M_{\rm gal}$ is higher in hot-gas poor than in hot-gas rich ellipticals (Fig. 4) implies that the former are more likely to fill any central core. Quantitatively, this result will depend on the properties of the cloud mass spectrum. In Section 4 we concluded that when the power-law slope α of the mass function of clouds is similar to the faint-end slope of the galaxy luminosity function, the mass of gas that can reach the centre, normalised to the galaxy mass $M_{\rm gal}$ is at least a factor of 3 higher in lower-mass ellipticals than in higher-mass ellipticals. This difference rises to at least a factor of 15 if $\alpha \sim 2$, as it would be if the cloud mass spectrum were the same as that of CDM halos. For very massive galaxies for which $M_{\rm min}$ could be almost as high as βM_* very little cold gas can reach the galaxy centre (see Section 4). So, we expect fainter galaxies to accumulate cold gas that supports central star formation, while the more massive galaxies can at most partially fill in the core created by dissipationless dynamics. The hypothesis that since its last major merger or accretion event every PLG has experienced an episode of central star formation from cold, rapidly rotating gas naturally explains all the observations listed in Section 5.1 under the headings (i) and (ii):

---

[4] The only outlier is NGC 4382, a core galaxy ($\gamma = 0.01$) with an estimated central age ~ 1.7 Gyr. We note that NGC 4382 has relatively low $L_{\rm X}/L_{\rm B}$ (Pellegrini 2005) and is characterised by atypical central SB profile and inner colour gradient (Lauer et al. 2005).

[5] Core scouring is not the only mechanism able to produce cored profiles: Nipoti, Londrillo & Ciotti (2006) showed that galaxies with SB profiles just like those of CGs can be obtained by a straightforward dissipationless collapse in the absence of a central BH.

[6] Lauer et al. (2005) conclude "Overall, the evidence is consistent with the binary BH core formation mechanism, but it is not a strong endorsement".

(ia) It is possible for a faint, gas-poor elliptical to be a CG galaxy simply because it has not encountered a source of cold gas since its last major merger. The brightest ellipticals have dense virial-temperature atmospheres, so no luminous galaxy should be a PLG.

(ib) The boxiness and slow rotation of CGs follows from the dominant role played by dissipationless dynamics in their formation.

(ic) If a prerequisite for being a CG is the ability to confine hot gas, these galaxies will be, or have been, the central galaxies of groups and clusters. When two groups merge, their central galaxies will merge, thus ensuring that the central galaxy of the new group is also a CG.

(id) We have seen that all X-ray luminous galaxies should be the central galaxies of groups or clusters. Such a galaxy can be a PLG only if its dense atmosphere built up *after* its last major merger. This is in principle possible but unlikely. When a small group falls into a rich cluster, it is possible that the central galaxy will be stripped of its dark halo before it is eaten by the central galaxy of the cluster. In this case we will observe a CG that is not X-ray luminous. There should be PLGs in all environments.

(iia) The late burst of star formation that filled in the post-merger core of a PLG can be expected to be metal-rich and enhance the galaxy's metallicity gradient.

(iib) The dynamical importance of rotation will increase as cold gas streams in, facilitating the formation of a central disk and/or a rapidly rotating kinematically decoupled core.

(iic) If infall continues long after the merger (Schweizer 1999) and cold gas can reach the centre, a blue nuclear cluster can form.

(iid) If stars cannot now form at the centres of CGs, the relative youth of the central stellar populations of PLGs is explained.

5.4 Mode of activity of the central black hole

We now show that our picture also explains the connections between galaxy morphology and active galactic nucleus (AGN) listed in Section 5.1 under the heading (iii).

There are two very different modes of BH accretion and feedback, usually referred to as "cold mode" (or QSO mode) and "hot mode" (or radio-mode) (e.g. Best et al. 2005; Binney 2005; Churazov et al. 2005; Hardcastle, Evans & Croston 2007; Sijacki et al. 2007). In short, these are the main properties of the two modes:

- *Cold mode*: the BH feeds from cold gas with $L \sim L_{\rm Edd}$, with most of the energy released going into photons (optical, UV, X-ray). The BH grows significantly in mass, and there is important attendant star formation. This mode is dominant at high redshift and leads to the correlation between BH and spheroid mass. The most extreme manifestations of cold mode accretion are luminous QSOs.
- *Hot mode*: the BH feeds from hot gas at $L \ll L_{\rm Edd}$, and most of the energy released is mechanical, being associated with bipolar flows, which generate significant radio emission. The BH mass does not increase significantly, and star formation is inhibited. The classic hot-mode accretor is Virgo A = M87 (Di Matteo et al. 2003), but FRI radio sources probably all belong to this class.

Cold-mode accretors can be either radio-loud or radio-quiet, while hot-mode accretors are invariably radio-loud.

In our picture all CGs must be hot-mode accretors, while PLGs can be either hot- or cold-mode accretors, depending on whether they happen to have encountered some cold gas recently. Items (iiia), (iiib) and (iiic) of Section 5.1 are consistent with this expectation, and taken together suggest that most PLGs are in fact accreting cold gas.

A possible explanation of the radio-loudness of CGs is the suggestion of Capetti & Balmaverde (2006) that a galaxy's merging history determines both the presence of the core and the spin of the BH, and that the latter controls radio-loudness (see also Wilson & Colbert 1995; Cen 2007; Sikora, Stawarz & Lasota 2007; Volonteri, Sikora & Lasota 2007). If BH spin were the only factor determining radio-loudness, the radio-loudness of a BH could only change slowly with time. Observations of micro-quasars show that a single source —regardless of whether it is powered by a BH or by a neutron star— often alternates short bursts of radio-loudness with longer periods of radio quiescence (Nipoti, Blundell & Binney 2005). In addition, the long-term time variability of central radio sources in galaxy clusters (once properly scaled for the BH mass) is consistent with that of microquasars (Nipoti & Binney 2005). These two pieces of evidence suggest that radio-loudness is more likely to be controlled by the accretion mode than by BH spin. The results of the present paper show that the observed radio properties of PLGs and CGs fit consistently in this scenario.

Thus a considerable body of observational evidence points to a scenario in which the ability of cold gas to survive evaporation from the hot ISM is responsible for determining both the inner stellar profiles of elliptical galaxies and the radio emission from their central supermassive BHs.

6 END OF THE BLUE CLOUD

As outlined in the Introduction, a robust bimodality is observed in the properties of galaxies, which in colour-magnitude diagrams are nicely segregated into a red sequence (extending to the brightest magnitudes) and a blue cloud (truncated at $\sim L_*$). These features, together with the shape of bright-end of the galaxy luminosity function, are hard to reproduce in standard galaxy formation models based on the proposal by Rees & Ostriker (1977) and White & Rees (1978) that galaxies form by cooling virial-temperature gas.

Until recently it has been widely assumed that during virialization of a dark-matter halo gas is heated to the virial temperature and that galaxies form through the cooling of this hot gas. However, both analytic and numerical results suggest that during virialization only a fraction of the gas is heated to the virial temperature, and that this fraction is negligible in halos less massive than a critical mass $M_{\rm crit} \approx 10^{12} M_\odot$ (Binney 1977; Birnboim & Dekel 2003; Keres et al.

2005; Dekel & Birnboim 2006). Moreover, as Binney (2004) first pointed out, observations of cooling flows suggest that heating by AGN-powered jets ensures that gas trapped at the virial temperature never cools. Hence this gas is not available for star formation, and galaxies can only go on forming stars and remain in the blue cloud to the extent that they can acquire cool gas. Hence the process studied above, of thermal evaporation of cold gas by hot, bears on the origin of the entire Hubble sequence as well as the morphological dichotomy of elliptical galaxies.

While there is now a wide measure of agreement that in very massive galaxies star formation is "quenched" through lack of cold gas, the mechanism responsible for cutting off the supply of cold gas is controversial. Dekel & Birnboim (2007) argue that gravitational heating alone suffices (see also Khochfar & Ostriker 2007). While the efficiency of gravitational heating undoubtedly rises with the clustering mass scale, several observations indicate that non-gravitational heating is important. Indeed studies of the temperature-luminosity correlation of diffuse X-ray sources has long provided strong evidence for powerful non-gravitational heating (Kaiser 1991; Ponman, Sanderson & Finoguenov 2003). Other indications are the small fraction of baryons contained in galaxies, both in groups like the MW and in rich clusters, the significant fraction of the products of nucleosynthesis that are in intracluster media (Renzini 1997), and the direct observation of massive outflows from star-forming galaxies at both small and high redshift (Strickland et al. 2004; Pettini et al. 2000).

The availability of non-gravitational heating is crucial because gravity alone will never drive gas *out* of dark matter halos, and the fact that at faint magnitudes the galaxy luminosity function falls further and further below the mass function of dark halos has long been attributed to the ability of non-gravitational heating to drive gas out of low-mass halos (White & Rees 1978; Dekel & Silk 1986). So it seems clear that energy released during star (and possibly black-hole) formation prevents virial temperature gas accumulating in low-mass halos. When cool gas falls into these systems it is not heated to the virial temperature, so star formation can continue in them.

It has been suggested that quasars are responsible for terminating star formation in their hosts (Springel, Di Matteo & Hernquist 2005). We feel this proposal is implausible for two reasons: (i) The abundant evidence for (a) an association between the masses of black holes and their host bulges, (b) the coincidence between the peaks in the cosmic star-formation rate and the quasar luminosity density, and (c) the rapidity of bulge formation, indicates that quasars are associated with rapid star formation, rather than quenching of star formation. (ii) Observations of disk galaxies imply that cold infall is a sustained process, while quasars flare up and then die. So while a quasar may clear its host of cold gas, it cannot be responsible for keeping the host clean after its death – which is the great majority of the host's life. In our view black holes have a vital role to play in quenching star formation, but their role is an indirect one: acting as thermostats for virial-temperature gas, which bears direct responsibility for quenching star formation. The connections between quasars and bulges arise because when cold gas is available on non-circular orbits (for example during a merger), bulge stars form rapidly on non-circular orbits and black holes accrete rapidly in an environment that causes energy released by accretion to be rapidly degraded into low-energy photons that produce only weak feedback on the interstellar medium (Sazonov et al. 2005).

When a halo reaches the critical mass $M_{\rm crit}$ two things happen almost simultaneously: (i) the fraction of infalling gas that stays below the virial temperature starts to dwindle, and (ii) the virial temperature rises above the temperature to which star and black-hole formation heat gas, so a hot atmosphere begins to accumulate – the temperature of this atmosphere is subsequently adjusted to the virial temperature by hot-mode accretion onto the black hole. We do not yet know how precise is the coincidence of the mass scales associated with the apparently independent processes (i) and (ii). However, it is does seem likely that this mass scale accounts for the upper limit to the luminosities of objects in the blue cloud, and that thermal evaporation plays a significant role in setting this limit. Semi-analytic models show that several features of the distribution of galaxies in colour, magnitude and redshift can be accounted for if there is a critical halo mass above which star-formation is quenched (e.g. Croton et al. 2006; Cattaneo et al. 2006; Dekel & Birnboim 2006).

A key object, that seems to be on the cusp of the transition across $M_{\rm crit}$ is the edge-on spiral galaxy NGC 5746. A *Chandra* observation shows that this galaxy is enveloped by a nearly spherical halo of X-ray emitting gas (Rasmussen et al. 2006). The authors suggest that star formation in the disk is sustained by cooling of this halo in the manner envisaged by White & Rees (1978), but it is hard to understand why cooling and star formation is not concentrated at the centre of the bulge, where the halo is densest and the cooling time shortest, rather than further out in the disk, nor how such a nearly spherical cloud could give rise to a disk in circular motion. It seems much more likely that in NGC 5746 we see the first stages in the growth of the body of trapped virial-temperature gas that will shortly quench star formation, causing the galaxy to move onto the red sequence.

The red sequence extends to faint magnitudes because galaxies hosted by halos that are much less massive than $M_{\rm crit}$ fall into halos of mass $M > M_{\rm crit}$ and then quickly become red because (i) their own cold gas is stripped out of them by a combination of ablation, thermal conduction and supernova-driven flows, and (ii) their prospects of accreting fresh cold gas are small given that they are now orbiting inside a halo of mass $M > M_{\rm crit}$ and moving too fast to merge with other galaxies, which anyway have little cold gas to offer. Postman et al. (2005) showed that the density-morphology relation is driven by the growth with density in the number of S0 galaxies at the expense of spirals, and Bedregal, Aragón-Salamanca & Merrifield (2006) and Barr et al. (2007) have recently proven beyond reasonable doubt that spiral galaxies passively fade into S0 galaxies, presumably as a result of gas-starvation. Another indication that many red-sequence galaxies orbit in more massive halos is the fact that they are preferentially found in dense environments, while blue-cloud galaxies typically reside in lower-density environments (e.g. Baldry et al. 2006).

In summary, a galaxy will move from the blue cloud to the red sequence *either* because it sits in a primary halo and the mass of this has just surpassed $M_{\rm crit}$, *or* because it starts to orbit sufficiently deeply in the potential of a primary halo with mass $> M_{\rm crit}$. From this hypothesis it should be possible to predict the luminosity functions of the blue cloud and the red sequence as functions of redshift, and the clustering properties of red-sequence galaxies. However, to make these predictions one needs both a detailed picture of the clustering of dark halos and the distribution of virial-temperature gas. The former could be taken from the halo model (Seljak 2000), but there is currently no obvious source, either theoretical or observational, from which to draw the latter: determining the distribution of hot gas observationally is hard because extended, low-density virial-temperature gas is a weak X-ray emitter and current X-ray detectors do not have useful velocity resolution. Building a model of the hot gas from cosmological simulations that include baryons is problematic because of the importance for gas of feedback from stars and AGN.

7 SUMMARY AND CONCLUSIONS

Cool gas is a fundamental ingredient for galaxy formation and evolution. Naturally, the study of cool gas in galaxies has been mainly focused on late-type galaxies, in which cool gas is most abundant. Early-type galaxies are rather poor in cool gas, but thanks to recent surveys, in CO (Sage, Welch & Young 2007), HI (Morganti et al. 2006; Oosterloo et al. 2007) and optical lines (Sarzi et al. 2006), we now have a detailed picture of the properties of the cool gas also in these systems. In elliptical galaxies such cool gas is immersed in a sea of plasma at the galaxy's virial temperature, and a long-standing question is how these two phases coexist and interact. In previous works evaporation of cool gas by thermal conduction from gas in the hot phase has been invoked in order to explain the shutdown of star formation in massive galaxies (Binney 2004; Dekel & Birnboim 2006) and the observed ionised-gas kinematics relative to that of the stars in early-type galaxies (Sarzi et al. 2007), but quantitative estimates of the importance of this process were lacking.

This paper gives a quantitative study of the evaporation of cold gas clouds by thermal conduction from the hot ISM. We focused on two classes of luminous elliptical galaxies, the low-mass (LM) and high-mass (HM) systems, both of which probably have potential wells deep enough to trap gas heated by star formation, but which differ in the densities of their virial-temperature atmospheres. We have shown that in the LM systems accreted cold gas is much more likely to feed central star formation than in the HM systems. This fact naturally explains the observed dichotomy between PLGs and CGs in central surface brightness profiles, X-ray luminosity, and activity of the central supermassive BH.

Our exploration is based on a rather simplified analytical model of the interaction between cold and hot gas, in which we account in detail only for thermal conduction and radiative cooling because we expect these to be the dominant physical processes. Ideally, the next step would be to explore the problem of cold-gas accretion and evaporation by the hot ISM using self-consistent three-dimensional hydrodynamical simulations. However, due to resolution limits, it appears difficult to describe numerically such a multiphase gas, even with state-of-the-art hydrodynamical simulations (e.g. Kaufmann et al. 2006; Bryan 2007, and references therein). Another useful step would be to add the results obtained here to semi-analytic models of galaxy formation (Bower et al. 2006; Cattaneo et al. 2006; Croton et al. 2006). Of course, a semi-analytic model is only as good as its input physics and such models are no substitute for ab-initio modelling from elementary physical principles.

Stripping and ablation of cold gas from galaxies that are orbiting in the potential well of a system that has abundant virial-temperature gas undoubtedly plays a large role in determining the morphology of galaxies and the extension of the red sequence to faint magnitudes. This process is closely related to the one quantified in this paper.

It now seems very likely that the central factor in dividing galaxies into the red sequence and the blue cloud is the existence of a critical halo mass above which gas accumulates at the virial temperature. What is still unclear is whether the supply of cold gas cuts off in galaxies associated with massive halos because infalling gas is then shock heated to the virial temperature (Dekel & Birnboim 2006), or because cold gas is evaporated and ablated by the hot gas (Binney 2004; Nipoti & Binney 2004). This paper shows that thermal evaporation is certainly a non-negligible process.

ACKNOWLEDGMENTS

We acknowledge helpful discussions with L. Ferrarese, A. Graham, S. Pellegrini, M. Sarzi, S. Tremaine and M. Volonteri. We thank the anonymous referee for a constructive report. CN is grateful to Merton College (Oxford) for hospitality.

REFERENCES

Balbus S., 1986, ApJ, 304, 787

Baldry I.K., Glazebrook K., Brinkmann J., Ivezić Ž, Lupton R.H., Nichol R.C., Szalay A.S., 2004, ApJ, 600, 681

Baldry I.K., Balogh M.L., Bower R.G., Glazebrook K., Nichol R.C., Bamford S.P., Budavari T., 2006, MNRAS, 373, 469

Balmaverde B., Capetti A., 2006, A&A, 447, 97

Barr J.M., Bedregal A.G., Aragon-Salamanca A., Merrifield M.R., Bamford S.P., 2007, A&A, 470, 173

Bedregal A.G., Aragón-Salamanca A., Merrifield M.R., 2006, MNRAS, 373, 1125

Begelman M.C., Blandford R.D., Rees M.J., 1980, Nature, 287, 307

Best P.N., Kauffmann G., Heckman T.M., Brinchmann J., Charlot S., Ivezić Ž, White S.D.M., 2005, MNRAS, 362, 25

Binney J., 1977, ApJ, 215, 483

Binney J., 2004, MNRAS, 347, 1093

Binney J., 2005, Phil. Trans. R. Soc. London, A, 363, 739

Binney J., Cowie L.L., 1981, ApJ, 247, 464

Binney J., Tremaine S., 1987, Galactic Dynamics, Princeton University Press, Princeton

Birnboim Y., Dekel A., 2003, MNRAS, 345, 349

Birzan L., Rafferty D.A., McNamara B.R., Wise M.W., Nulsen P.E.J., 2004. ApJ, 607, 800

Blanton M.R. et al., 2003, ApJ, 594, 186

Böhringer H., Fabian A.C., 1989, MNRAS, 237, 1147

Bower R.G., Benson A.J., Malbon R., Helly J.C., Frenk C.S., Baugh C.M., Cole S., Lacey C.G., 2006, MNRAS, 370, 645

Bryan G.L., 2007, EAS Publications Series, Volume 24, pp.77-88, Eds. Emsellem, Wozniak, Massacrier, Gonzalez, Devriendt, Champavert (arXiv:0707.1856v1)

Capetti A., Balmaverde B., 2006, A&A, 453, 27

Cattaneo A., Dekel A., Devriendt J., Guiderdoni B., Blaizot J., 2006, MNRAS, 370, 1651

Churazov E., Sazonov S., Sunyaev R., Forman W., Jones C., Böhringer H., 2005, MNRAS, 363, L91

Cen R., 2007, preprint (astro-ph/0702660)

Côté P. et al., 2006, ApJS, 165, 57

Cowie L.L., McKee C.F., 1977, ApJ, 211, 135

Cowie L.L., Songaila A., 1977, Nature, 266, 501

Croton D.J. et al., 2006, MNRAS, 365, 11

David L.P., Jones C., Forman W., Vargas I.M., Nulsen P., 2006, ApJ, 653, 207

Dekel A., Birnboim Y., 2006, MNRAS, 368, 2

Dekel A., Birnboim Y., 2007, preprint (arXiv:0707.1214v1)

Dekel A., Silk J., 1986, ApJ, 303, 39

de Ruiter H.R., Parma P., Capetti A., Fanti R., Morganti R., Santantonio L., 2005, A&A, 439, 487

Di Matteo T., Allen S.W., Fabian A.C., Wilson A.S., Young A.J., 2003, ApJ, 582, 133

Driver S.P. et al., 2006, MNRAS, 368, 414

Ebisuzaki T., Makino J., Okumura S.K., 1991, Nature, 354, 212

Ellis S.C., O'Sullivan E., 2006, MNRAS, 367, 627

Faber S. et al., 1997, AJ, 114, 1771

Fraternali F., Binney J., 2006, MNRAS, 366, 449

Ferrarese L. et al., 2006, ApJS, 164, 334

Fukazawa Y., Botoya-Nonesa J.G., Pu J., Ohto A., Kawano N., 2006, ApJ, 636, 698

Graham A.W., Erwin P., Trujillo I., Asensio Ramos A., 2003, AJ, 125, 2951

Graham A.W., 2004, ApJ, 613, L33

Hardcastle M.J., Evans, D.A., Croston J.H., 2007, MNRAS, 376, 1849

Humphrey Ph.J., Buote D.A., Gastaldello F., Zappacosta L., Bullock J.S., Brighenti F., Mathews W.G., 2006, ApJ, 646, 899

Irwin J.A., Sarazin C.L., 1996, ApJ, 471, 683

Kaiser N., 1991, ApJ, 383, 104

Kaufmann T.,Mayer L., Wadsley J., Stadel J., Moore B., 2006, MNRAS, 370, 1612

Keres D., Katz N., Weinberg D.H., Davé R., 2005, MNRAS, 363, 2

Khochfar S., Ostriker J.P., 2007, preprint (arXiv:0704.2418v1)

Kormendy J., Bender R., 1996, ApJ, 464, L119

Laine S., van der Marel R.P., Lauer T.R., Postman M., O'Dea C.P., Owen F.N., 2003, AJ, 125, 478

Landau L.D., Lifshitz E.M., 1959, Fluid mechanics. Course of theoretical physics, Pergamon Press, Oxford

Larson R.B., 1974, MNRAS, 166, 585

Lauer T. et al., 1995, AJ, 110, 2622

Lauer T. et al., 2005, AJ, 129, 2138

Lauer T. et al., 2007, ApJ, 664, 226

Magorrian J. et al., 1998, AJ, 115, 2285

Makino J., Ebisuzaki T., 1996, ApJ, 465, 527

Marconi A., Hunt L.K., 2003, ApJ, 589, L21

Mathews W.G., Brighenti F., 2003, ARA&A, 41, 191

McDermid R.M. et al., 2006, MNRAS, 373, 906

McKee C.F., Cowie L.L., 1977, ApJ, 215, 213

Merritt D., 2006, Rept. Prog. Phys. D69, 2513 (astro-ph/0605070)

Milosavljevic M., Merritt D., 2001, ApJ, 563, 34

Milosavljevic M., Merritt D., Rest A., van den Bosch F.C., 2002, MNRAS, 331, L51

Morganti R. et al., 2006, MNRAS, 371, 157

Nipoti C., Binney J., 2004, MNRAS, 349, 1509

Nipoti C., Binney J., 2005, MNRAS, 361, 428

Nipoti C., Blundell K.M., Binney J., 2005, MNRAS, 361, 633

Nipoti C., Londrillo P., Ciotti L., 2006, MNRAS, 370, 681

Oosterloo T., Morganti R., Sadler E.M., van der Hulst J.M., Serra, P., 2007, A&A, 465, 787

O'Sullivan E., Sanderson A.J.R., Ponman T.J., 2007, MNRAS, in press (arXiv:0707.1879v1)

Pellegrini S., 1999, A&A, 351, 487

Pellegrini S., 2005, MNRAS, 364, 169

Pettini M., Steidel C.C., Adelberger K.L., Dickinson M., Giavalisco M., 2000, ApJ, 528, 96

Ponman T.J., Sanderson A.J.R., Finoguenov A., 2003, MNRAS, 343, 331

Postman, M. et al. 2005, ApJ. 623, 721

Quinlan G.D., Hernquist L., 1997, New Astron., 2, 533

Randall S.W., Sarazin C.L., Irwin J.A., 2006, ApJ, 636, 200

Rasmussen J., Sommer-Larsen J., Pedersen K., Toft S., Benson A., Bower R.G., Olsen L.F., 2006, peprint (arXiv:astro-ph/0610893v1)

Ravindranath S., Ho L.C., Peng C.Y., Filippenko A.V., Sargent W.L.W., 2001, AJ, 122, 653

Renzini A., 1997, ApJ, 488, 35

Rest A., van den Bosch F.C., Jaffe W., Tran H., Tsvetanov Z., Ford H.C., Davies J., Schafer J., 2001, AJ, 121, 2431

Rees M.J., Ostriker J.P., 1977, MNRAS, 179, 541

Sage L.J., Welch G.A., Young L.M., 2007, ApJ, 657, 232

Sarzi M. et al., 2006, MNRAS, 366, 1151

Sarzi M. et al., 2007, New Astron Rev., 51, 18

Sazonov S.Yu., Ostriker J.P., Ciotti L., Sunyaev R.A., 2005, MNRAS, 358, 168

Schechter, P., 1976, ApJ, 203, 297

Schweizer, F., 1999, ASpS, 267, 299

Seljak, U., 2000, MNRAS, 318, 203

Sersic J.L., 1968, Atlas de galaxias australes. Observatorio Astronomico, Cordoba

Sijacki D., Springel V., Di Matteo T., Hernquist L., 2007, submitted to MNRAS (arXiv:0705.2238v1)

Sikora M., Stawarz L., Lasota J.-P., 2007, ApJ, 658, 815

Spitzer L., 1956, ApJ, 124, 20

Spitzer L., 1962, Physics of Fully Ionized Gases. Wiley-Interscience, New York

Springel V., Di Matteo T., Hernquist L., 2005, ApJ, 620, L79

Strickland D.K., Heckman T.M., Colbert E.J.M., Hoopes C.G., Weaver K.A., 2004, ApJS, 151, 193

Tribble P.C., 1989, MNRAS, 238, 1247

Trujillo I., Erwin P., Asensio Ramos A., Graham A.W., 2004, AJ, 127, 1917

Volonteri M., Madau P., Haardt F., 2003, ApJ, 593, 661

Volonteri M., Sikora M., Lasota J.-P., 2007, ApJ in press (arXiv:0706.3900v1)
White S.D.M., Rees M.J., 1978, MNRAS, 183, 341
Wilson A.S., Colbert E.J.M., 1995, ApJ, 438, 62

APPENDIX A: EVAPORATION OF SPHEROIDAL CLOUDS

A1 Saturation

The classical heat flux (equation 1) is derived under the assumption that the mean free path of the electrons is small with respect to the temperature scale height $T/|\nabla T|$. When this condition is not satisfied, typically for very high electron temperature and/or very low electron density, equation (1) does not hold and the heat flux is said to be *saturated.* As a discriminant of whether the heat flux in a plasma is saturated, Cowie & McKee (1977) introduced the parameter $\sigma \equiv q_{\rm cl}/q_{\rm sat}$, where $q_{\rm cl} = \kappa(T)|\nabla T|$ is the modulus of the classical heat flux, and the modulus of the saturated heat flux is

$$q_{\rm sat} = 5 f^{1/2}\phi_{\rm sat}\rho c_{\rm s}^3, \tag{A1}$$

where $\phi_{\rm sat} \sim 1$ is a dimensionless parameter, ρ is the mass density of the gas, $c_{\rm s} = \sqrt{P/\rho} = \sqrt{k_{\rm B}T/\mu m_{\rm p}}$ is the isothermal sound speed, and P is the pressure. The quantity $q_{\rm sat}$ in equation (A1) differs from that in Cowie & McKee (1977) for the presence of $f^{1/2}$, which we included to account for the effects of magnetic fields (see Cowie & McKee 1977; Balbus 1986, for a discussion). The critical value that separates the two regimes is $\sigma \sim 1$: for $\sigma \ll 1$ the heat flux is unsaturated, while for $\sigma \gg 1$, equation (A1) applies. In the case of the evaporation of a cloud modelled as a prolate or oblate spheroid we get

$$\sigma = f^{1/2}\sigma_0 g(u,v,\epsilon)\frac{P_{\rm ism}}{P(u)}, \tag{A2}$$

where $P_{\rm ism} = \lim\limits_{u\to\infty} P(u)$ is the ISM pressure,

$$\begin{aligned}\sigma_0 &= \frac{2\kappa_0 T_{\rm ism}^{7/2}}{25\phi_{\rm sat}\rho_{\rm ism}c_{\rm s,ism}^3 a} \qquad\qquad (A3)\\ &\simeq \frac{4.5\times10^{-4}}{\phi_{\rm sat}}\left(\frac{T_{\rm ism}}{10^7\,{\rm K}}\right)^2\left(\frac{n_{\rm e,ism}}{\rm cm^{-3}}\right)^{-1}\left(\frac{a}{\rm kpc}\right)^{-1}.\end{aligned}$$

is the saturation parameter[7] (Cowie & McKee 1977), and (u,v) are the spheroidal coordinates introduced in Section 2. Here $\rho_{\rm ism}$ and $c_{\rm s,ism}$ are the mass density and isothermal sound speed of the ISM, and we used $\rho_{\rm ism} \simeq 1.15 m_{\rm p} n_{\rm e,ism}$ and $\phi_{\rm sat} \sim 1$. The dimensionless function $g(u,v,\epsilon)$ in the oblate case is

$$g(u,v,\epsilon) = -\frac{[\theta(u_0)-\theta(u)]^{1/5}}{2\left[\theta(u_0)-\frac{\pi}{4}\right]^{6/5}\cosh u\sqrt{\sinh^2 u+\cos^2 v}}, \tag{A4}$$

where $\theta(x) \equiv \arctan[\tanh(x/2)]$, while in the prolate case

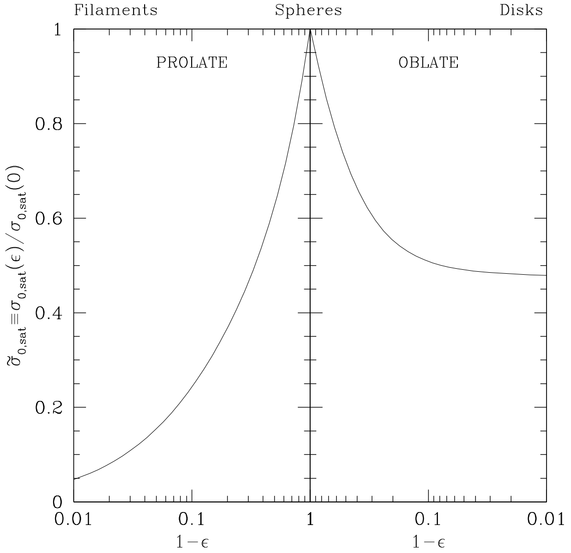

Figure A1. Top: $\tilde\sigma_{0,\rm sat}$ as a function of the ellipticity ϵ of prolate (left panel) and oblate (right panel) clouds.

$$g(u,v,\epsilon) = -\frac{[\gamma(u_0)-\gamma(u)]^{1/5}}{[\gamma(u_0)]^{6/5}\sinh u\sqrt{\sinh^2 u+\sin^2 v}}, \tag{A5}$$

where $\gamma(x) \equiv \ln[\tanh(x/2)]$, and we recall that $u_0 = {\rm arctanh}(1-\epsilon)$.

The term $P_{\rm ism}/P(u)$, appearing in equation (A2), is expected to be of the order of unity or smaller, because dense clouds tend to be overpressured with respect to their environments, and the pressure is approximately constant throughout the flow if the Mach number is not large (Cowie & McKee 1977). While in the case of a spherical cloud of radius a the condition for saturation $[\max(\sigma) > 1]$ is equivalent to $\sigma_0 \gtrsim 1$ (Cowie & McKee 1977), for significantly non-spherical prolate and oblate clouds this transition occurs at a critical value of $\sigma_0 \ll 1$, because the geometry implies stronger temperature gradients near the equatorial plane in the oblate case and near the symmetry axis in the prolate case. This is reflected in the behaviour of the function $g(u,v,\epsilon)$ appearing in equation (A2): for $\epsilon \to 1$ the function $g(u,v,\epsilon)$, at fixed v, has a maximum that significantly exceeds unity, especially for $v \to \pi/2$ (oblate) and $v \to 0$ (prolate). However, even for σ_0 significantly larger than the critical value, the heat flux is overestimated only in a small region around $v = \pi/2$ (oblate) or $v = 0$ (prolate), which gives a negligible contribution to the heat flow. If the surface of the cloud is $S_{\rm tot}$, and the surface in which saturation occurs is $S_{\rm sat}$, the fraction of the heat flow that is overestimated is $\zeta \equiv \int_{S_{\rm sat}} \mathbf{q}_{\rm cl}\cdot d^2\mathbf{S}/\int_{S_{\rm tot}} \mathbf{q}_{\rm cl}\cdot d^2\mathbf{S}$, where $d^2\mathbf{S}$ is the area element. Integration gives $\zeta = 1-\cos v_{\rm sat}$ (oblate), $\zeta = \cos v_{\rm sat}$ (prolate), where $v_{\rm sat}$ is the value of v at which the transition between classical and saturated heat flux occurs. As long as $\zeta \ll 1$, the unsaturated computation still yields a good approximation of the actual heat flow. So, we define a reference value of the saturation parameter $\sigma_{0,\rm sat}$ (depending on ϵ) such that $\zeta < 1/3$ for $\sigma_0 < \sigma_{0,\rm sat}$. $\tilde\sigma_{0,\rm sat} \equiv \sigma_{0,\rm sat}(\epsilon)/\sigma_{0,\rm sat}(0)$ as a function of ϵ is plotted in Fig. A1. The mass loss rate $\dot M_{\rm sat}$ for saturated heat flux can be computed analytically only for spherically symmetric clouds (Cowie & McKee 1977), being

---

[7] Our definition of σ_0 differs from that in (Cowie & Songaila 1977) by a factor $\cosh u_0$, so that in the limit $\epsilon \to 0$ we recover the definition of Cowie & McKee (1977) for a spherical cloud of radius a.

$$\dot{M}_{\rm sat} = 4\pi f^{1/2} a^2 \rho_{\rm ism} c_{\rm s,ism} \phi_{\rm sat} F(\sigma_0), \tag{A6}$$

with $F(\sigma_0) \simeq 2.73\sigma_0^{3/8}$ if $\phi_{\rm sat} \sim 1$, where we included the factor $f^{1/2}$ to account for the effects of magnetic fields.

A2 Radiation

McKee & Cowie (1977) showed that a spherically symmetric cold cloud immersed in a hot ($T_{\rm ism} \gtrsim 10^5\,{\rm K}$) ambient medium is radiatively stabilised when $\sigma_0 \simeq 0.027/\phi_{\rm sat}$. For given physical properties of the ambient medium, this condition is satisfied when the cloud radius is $a_{\rm rad}$ given in equation (9), which is approximately valid also in the oblate case (Cowie & Songaila 1977). In Nipoti & Binney (2004) we computed the critical length $l_{\rm crit}$ of radiatively stabilised filaments of cool gas immersed in a hot medium. So, for very elongated prolate clouds ($\epsilon \to 1$) an estimate of the critical size is

$$a_{\rm rad} \simeq \frac{l_{\rm crit}}{2} \simeq 0.07 f^{1/2} \lambda^{1/2} \left(\frac{T_{\rm ism}}{10^7\,{\rm K}}\right)^{7/4} \left(\frac{n_{\rm e,ism}}{{\rm cm}^{-3}}\right)^{-1} {\rm kpc}, \tag{A7}$$

where $0.08 \lesssim \lambda(T_{\rm ism}) \lesssim 0.37$ for $10^6 \lesssim T_{\rm ism}/\,{\rm K} \lesssim 10^8$ (Nipoti & Binney 2004). This results has been obtained in cylindrical symmetry for clouds with electron temperature $T_{\rm c} \sim 10^4\,{\rm K}$, assuming constant pressure in the interface. An approximated estimate of the evaporation time for cylindrical clouds of length $l < l_{\rm crit}$ is $t_{\rm ev,cyl} \sim (l/l_{\rm crit})^2 t_{\rm cool}$, where $t_{\rm cool}$ is the cooling time (Nipoti & Binney 2004). We verified that in the temperature range $10^6 - 10^7\,{\rm K}$ $t_{\rm ev,cyl} \sim t_{\rm ev}$, where $t_{\rm ev}$ is the evaporation time of a cold prolate cloud with $\epsilon \sim 0.98$, and equations (A7) for filaments and (9) for spheres yield to values of $a_{\rm rad}$ within a factor of two. This suggests that we can safely assume that equation (9) gives an approximated estimate of $a_{\rm rad}$ also for prolate clouds.

APPENDIX B: DRAG FORCE

Beside gravity, a cloud of cold gas infalling with velocity $\mathbf{v}$ through a galaxy's ISM experiences the drag force

$$\mathbf{F}_{\rm drag} = -\frac{1}{2} C S \rho_{\rm ism} v^2 \frac{\mathbf{v}}{v}, \tag{B1}$$

where S is the cloud cross-section, $\rho_{\rm ism}$ is the density of the ambient medium at the position of the cloud, and C is the drag coefficient, which depends on the Reynolds number R (e.g. Landau & Lifshiz 1959). In our applications $R \ll 10^5$, and we crudely assume $C(R) = 24/R$ for $R < 48$ and $C(R) = 0.5$ for $R \geq 48$.

To estimate the effect of the drag force on the dynamics of the clouds we consider here the simple case of a spherical cloud of mass M infalling radially in the model galaxies LM and HM described in Section 3. Integrating the equation of motion

$$\ddot{r} = -\frac{G M_{\rm dyn}(r)}{r^2} + \frac{1}{2M} C(r) S(r) \rho_{\rm ism}(r) \dot{r}^2 \tag{B2}$$

between r and 0 with $v(r) = 0$, we obtain a dynamical time $t_{\rm dyn}(M, r)$. We note that at fixed mass, the cross-section depends on r because the cloud density does (see Section 2.1). The star-formation mass $M_{\rm sf}$ is such that $t_{\rm ev}(M_{\rm sf}, r) = t_{\rm dyn}(M_{\rm sf}, r)$. We found that the values of $M_{\rm min} = \max_{r>0} M_{\rm sf}(r)$ obtained considering equation (B2) are larger than those obtained in the absence of the drag force by $10-15$ per cent in the model galaxies LM and HM. We conclude that neglecting the effect of drag implies only a modest underestimation of the value of the minimum mass $M_{\rm min}$.

This paper has been typeset from a TEX/ LATEX file prepared by the author.